Korean J. of Chem. Eng., 9(4), 199-205 (1992)

MATHEMATICAL MODELLING OF A TWIN-ROLL STRIP CASTING PROCESS WITH TURBULENT FLOW – ON MOLTEN METAL FLOWFIELD –

Sung-Woo Lee

Machinery and Electronics Research Institute, Samsung Heavy Industries, 69, Sinchon-Dong, Changwon, Kyungnam 641-370, Korea

(*Received 16 June 1992 • accepted 19 November 1992*)

Abstract—A computer model has been developed for describing the flowfield of molten metal in the twin roll strip casting process with turbulent flow. The formulation of the twin roll strip casting process was based on the turbulent Navier-Stokes equation in which allowance was made for the spatially distributed turbulent velocity field of molten metal. The equations were simplified to those for axisymmetrical flowfields and an outline of the computational approach was also given. The calculation of turbulent properties using the standard two equation k-ε turbulence model has been applied, and predicted results are presented. Also, it was found that turbulent flowfields with a recirculating zone are located in the vicinity of the middle of the rotating bank of molten metal. The size of the recirculating zone with fixed geometry configuration decreases with increasing inlet flow rate.

INTRODUCTION

If sheet or strip (thickness<6 mm) can be produced directly from the molten metal by combining the casting and hot rolling into a single casting process just as a replacement for conventional continuous casting machines, the costly intermediate stages of ingot casting, primary rolling, reheating and some secondary rolling will be eliminated, and there can be substantial savings of capital, energy, operations, and labour [1-4]. Although the idea of casting directly between cooled rotating rollers was first proposed by Sir Henry Bessemer in 1891 [5], it has only in recent years been put into practice.

The principles of the twin-roll casting process are shown in Fig. 1. The casting procedure for steel strips has been operated using twin internally water-cooled copper alloy rollers. Molten metal is provided by a tundish or headbox and kept at a predetermined degree of superheat in the tundish. The molten stream of metal is fed through the fabricated ceramic nozzle passage as a submerged entry nozzle and between the rotating rollers. The rapidly solidified strips are carried by the rollers out of the nip. Understanding of the fundamental phenomena of the mechanisms responsible for the behaviour of molten metal flowfields in the process is limited, but such knowledge is exten-

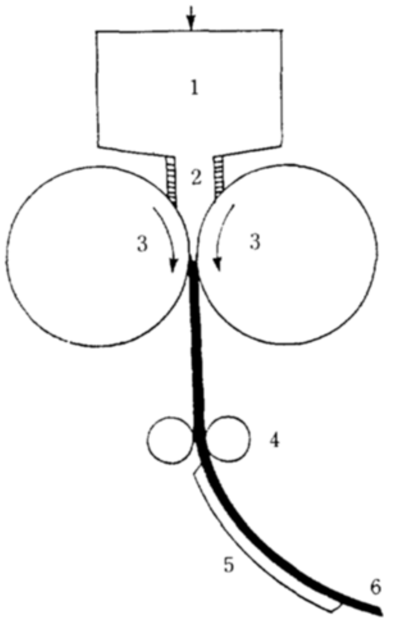

Fig. 1. Schematic description of a twin-roll strip casting process.

1. Ladle or tundish
2. Nozzle
3. Twin-rollers
4. Supporting rollers
5. Slide
6. Cast strip

sively exploited to enhance the optimal operating condition and process development. But, in this process, direct measurements of the flowfields are very difficult because the flowfield of molten metal is opaque and high temperature. The experimental study of fluid flow for molten metal behaviour is difficult to perform and is subject to a high degree of uncertainty and inaccuracy. As such the fluid flow will exhibit complexity, strong turbulence and scalar transport, which can be best resolved through a mathematical modelling approach for visualising the flowfields. Although some mathematical modelling of the process has been done [6-8], no model has yet appeared in which the turbulent nature of the flow is addressed. Analysis of the turbulent flow field in this configuration could be very important for the optimum design and development of this process for quantity production of strip. As a starting point, this model treats the flow as isothermal and neglects the solidification because the shell thickness solidified is much smaller than the region of molten flowfield.

The results obtained provide a quantitative relationship between the principal parameters, such as flow rate, roll spacing and width of the inlet nozzle, with special attention to the starting point of strip production.

MATHEMATICAL FORMULATION

1. Problem Description and Governing Equations

As mentioned before, this mathematical modelling assumes the flow as isothermal and neglects the solidification process. It is expected that the formation of solid layers on the rollers will have a small effect on the main flow in the recirculating bank of molten steel.

An idealized model geometry with the coordinate system is schematically shown in Fig. 2 with the control volume indicated by the dotted line. The molten metal stream of width 2W is fed from upstream into the gap of the twin counter rotating rollers, each having a roll speed Ω. The governing equations to describe the turbulent flow field of molten metal in this system can be expressed by a Reynolds decomposition and time-averaging of the instantaneous equations [9-11].

In Cartesian tensor notation, the equations which represent the conservation of mass and momentum are as follows:

$$\frac{\partial}{\partial x_i}(\rho u_i)=0 \tag{1}$$

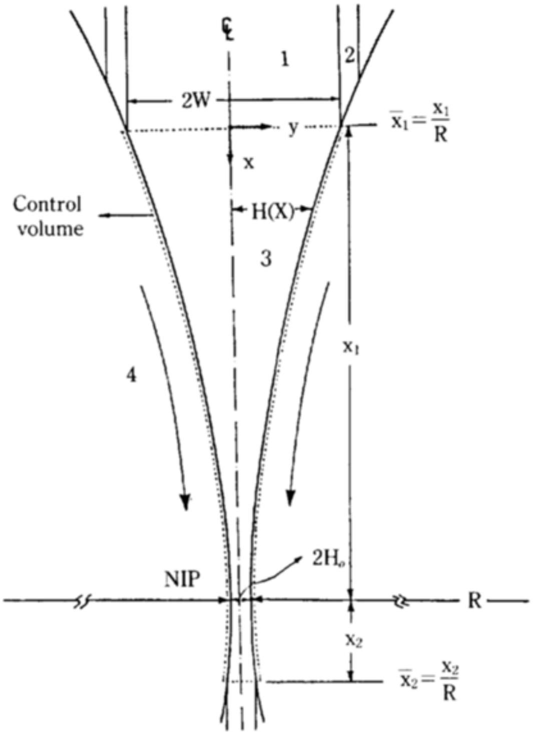

Fig. 2. Schematic representation of twin-roll strip casting process for a mathematical modelling.
1. Molten metal stream 2. Nozzle
3. Rotating bank 4. Twin-roller

$$\frac{\partial}{\partial x_j}(\rho u_i u_j)=-\frac{\partial P}{\partial x_i}+\frac{\partial}{\partial x_j}\left[\mu\left(\frac{\partial u_j}{\partial x_i}+\frac{\partial u_i}{\partial x_j}\right)\right]-\frac{\partial R_{ij}}{\partial x_j} \tag{2}$$

where R_{ij} is a tensor having both viscous and Reynolds stress parts.

These governing equations are assumed to be adequately represented by introducing the following simplifications for this system:

(1) the flowfield can be taken to be 2-dimensional axi-symmetric, incompressible and isothermal;

(2) the lubrication approximation may be used to describe the divergent flow beyond the nip;

(3) the rollers are not deformable and are both rotating at the same speed;

(4) there is no slip between the molten metal and the rotating rollers.

Here the standard k-ε turbulence model [12] is employed to characterize the effects of turbulence with the Reynolds stress tensor R_{ij}.

The effective viscosity, μ_e, is defined as the sum of a turbulent viscosity μ_t and the molecular viscosity μ:

Table 1. k-ε model constants [12]

C_1	C_2	C_D	σ_k	σ_ε
1.45	1.92	0.09	1.0	$K^2/(C_2-C_1)^{0.5}$

$$\mu_e=\mu_t+\mu \tag{3}$$

The turbulent viscosity, in contrast to the molecular viscosity, is not a fluid property but depends strongly on the state of turbulence and is defined by

$$\mu_t=C_D\rho k^2/\varepsilon \tag{4}$$

The quantities k and ε are obtained from the solution of their own transport equations which take the form: Turbulent kinetic energy,

$$\frac{\partial}{\partial x}(\rho uk)+\frac{\partial}{\partial y}(\rho vk) =\frac{\partial}{\partial x}\left(\frac{\mu_e}{\sigma_k}\frac{\partial k}{\partial x}\right)+\frac{\partial}{\partial y}\left(\frac{\mu_e}{\sigma_k}\frac{\partial k}{\partial y}\right)+G_k-\rho\varepsilon C_D \tag{5}$$

Its dissipation rate,

$$\frac{\partial}{\partial x}(\rho u\varepsilon)+\frac{\partial}{\partial y}(\rho v\varepsilon) =\frac{\partial}{\partial x}\left(\frac{\mu_e}{\sigma_\varepsilon}\frac{\partial \varepsilon}{\partial x}\right)+\frac{\partial}{\partial y}\left(\frac{\mu_e}{\sigma_\varepsilon}\frac{\partial \varepsilon}{\partial y}\right)+C_1\frac{\varepsilon}{k}G_k-C_2\rho\frac{\varepsilon^2}{k} \tag{6}$$

where, $S_u=\frac{\partial}{\partial x}\left(\mu_e\frac{\partial u}{\partial x}\right)+\frac{\partial}{\partial y}\left(\mu_e\frac{\partial v}{\partial x}\right)$ and

$$S_v=\frac{\partial}{\partial x}\left(\mu\frac{\partial u}{\partial y}\right)+\frac{\partial}{\partial y}\left(\mu_e\frac{\partial v}{\partial y}\right).$$

and the term G_k is the generation of turbulence, given by

$$G_k=\mu_t\left[2\left\{\left(\frac{\partial u}{\partial x}\right)^2+\left(\frac{\partial v}{\partial y}\right)^2\right\}+\left(\frac{\partial u}{\partial y}+\frac{\partial v}{\partial x}\right)^2\right] \tag{7}$$

Numerical values for the turbulence model constants appearing in Eqs. (4) to (6) are presented in Table 1.

In the Table 1, K is the von Kárman constant taken to be equal to 0.4187. Although the flowfields in this work will be predicted by the k-ε model, it is known [13] that this model has limitations in describing turbulence quantities. Improvement of the k-ε model or the use of more advanced Reynolds stress models is necessary for better prediction of turbulent flows for a rotating roller.

2. Boundary Conditions

The following boundary conditions were used for the numerical simulation of this turbulent flow field.

(1) At the inlet from the nozzle.

$$u=u_{in},\ v=0,$$
$$k_{in}=b(u_{in})^2,$$
$$\varepsilon_{in}=C_D^{3/4}k_{in}^{3/2}/(2W)$$

(2) At the outlet from the nip point,

$$v=0,\ \frac{\partial k}{\partial x}=0,\ \frac{\partial \varepsilon}{\partial x}=0$$

(3) At the axis,

$$v=0,\ \frac{\partial u}{\partial y}=0,\ \frac{\partial k}{\partial y}=0,\ \frac{\partial \varepsilon}{\partial y}=0$$

(4) At the roll surface,

$$u=u_r=\Omega[R^2-(x_1-x)^2]^{1/2},$$
$$v=v_r=u_r\frac{dH}{dx},$$
$$k=0,\ \varepsilon=0,\ \mu_t=0$$

where u_r and v_r are the velocity components of the roll surface in the x and y direction respectively.

In this system, in order to avoid using a fine grid near walls, where steep cross flow gradients exist, wall functions are used [12].

The u-component of velocity is then readjusted slightly at each iteration so as to ensure overall mass conservation as compared with inlet flow.

3. Numerical Solution Procedure

For this system, the time-averaged transport equations for continuity, momentum, turbulent kinetic energy, k, and its dissipation rate, ε, can be expressed in the following generalized variable form:

$$\frac{\partial}{\partial x}(\rho u\Phi)+\frac{\partial}{\partial y}(\rho v\Phi) =\frac{\partial}{\partial x}\left(\Gamma_\Phi\frac{\partial \Phi}{\partial x}\right)+\frac{\partial}{\partial y}\left(\Gamma_\Phi\frac{\partial \Phi}{\partial y}\right)+S_\Phi \tag{8}$$

where Γ_Φ and S_Φ denote the local exchange coefficient of variable Φ, and the terms that are not included in convection and diffusion terms. For different variables, Γ_Φ and S_Φ have different contents. The particular Γ_Φ and S_Φ expressions were given in Table 2.

For incompressible fluid between rotating roller, the continuity and momentum equations are transformed to a general curvilinear coordinate system as the procedure is well shown in reference [14, 15]. Two main features of the solution method used here are employment of the finite volume formulation and the algorithm SIMPLE (Semi-Implicit Method for Pressure Linked Equations) [16]. The representation of equation for Φ= u, v, p, k and ε is then solved by the algorithm

Table 2. The form of the source term in the general equation for Φ, Eq. (8)

Conserved property	Φ	Γ_Φ	S_Φ
Continuity	1	0	0
x-momentum	u	μ_e	$-\frac{\partial P}{\partial x}+\frac{\partial}{\partial x}\left(\mu_e\frac{\partial u}{\partial x}\right)+\frac{\partial}{\partial y}\left(\mu_e\frac{\partial v}{\partial x}\right)$
y-momentum	v	μ_e	$-\frac{\partial P}{\partial y}+\frac{\partial}{\partial x}\left(\mu_e\frac{\partial u}{\partial y}\right)+\frac{\partial}{\partial y}\left(\mu_e\frac{\partial v}{\partial y}\right)$
kinetic energy	k	μ_e/σ_k	$G_k-\rho\varepsilon C_D$
dissipation rate	ε	μ_e/σ_ε	$\frac{\varepsilon}{k}(C_1G_k-C_2\rho\varepsilon)$

where, $G_k=\mu_e\left[2\left(\frac{\partial u}{\partial x}\right)^2+2\left(\frac{\partial v}{\partial y}\right)^2+\left(\frac{\partial u}{\partial y}+\frac{\partial v}{\partial x}\right)^2\right]$

Table 3. Numerical values of parameters used in this computation of the twin-roll strip casting process

R radius of rotating roll, m	0.3
H_o roll-spacing, m	1, 1.5($\times 10^{-3}$)
W nozzle width, m	1.5, 3($\times 10^{-2}$)
ρ density of molten steel, kg/m^3	7200
μ molecular viscosity of molten steel, kg/ms	6.4×10^{-3}

SIMPLE. The iterative method of solution employed is a double sweep of Tri-Diagonal Matrix Algorithm (TDMA). The detailed description of the particular solution procedure employed here is presented in reference [16]. The system parameters and material properties used in the calculation are given in Table 3. The solution was considered to be converged if the cumulative sum of the absolute residuals throughout the field for all variables did not exceed 0.5 percent of the inlet flow rate of the corresponding variable.

4. Computed Results and Discussion

The primary purpose of the computation was to predict the turbulent velocity fields from the inlet nozzle to the outlet from the rotating rollers. In presenting the computed results, we shall show a number of velocity vector plots and some figures of turbulence characteristics. The intention here is to illustrate the sensitivity of the system to the values of various operating parameters.

The calculated velocity vectors for $\Omega=150$ rpm, $W=1.5\times10^{-2}$m and $H_o=1.5\times10^{-3}$m are shown as a function of the inlet velocity, u_{in}, in Fig. 3, respectively.

The flow patterns in the molten metal pool show that there is a large region of recirculating flow centred in the middle of the rotating bank of the molten metal pool. Thus, near the mid-plane fluid moves away from the nip of the rollers because the velocity components are negative but near the roll surface the velocity components are positive and the fluid moves toward the nip. Also, it can be seen that the molten metal stream exhibits a jet-like character in the vicinity of the roll surface with the axial velocity component having a parabolic profile. As seen in Fig. 3(d), the recirculating zone disappears from the rotating bank when a high inlet velocity is introduced, which generates a large normal axial pressure gradient.

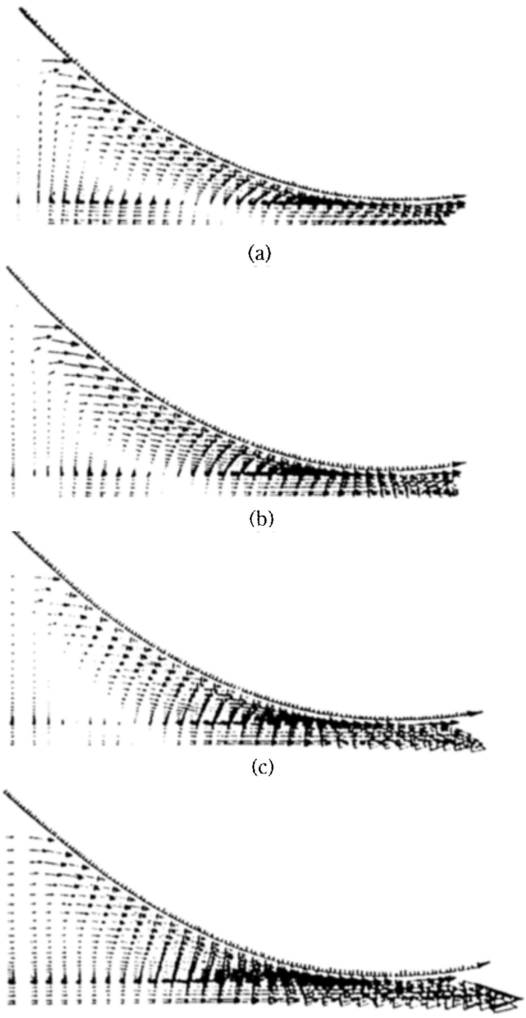

(a) (b) (c) (d)

Fig. 3. Predicted velocity fields corresponding to various inlet velocity u_{in} for $\Omega=150$ rpm, $W=1.5\times10^{-2}$ m and $H_o=1.5\times10^{-3}$ m.
(a) $u_{in}=0.355$ m/s, (b) $u_{in}=0.555$ m/s, (c) $u_{in}=0.8$ m/s, (d) $u_{in}=1.2$ m/s.

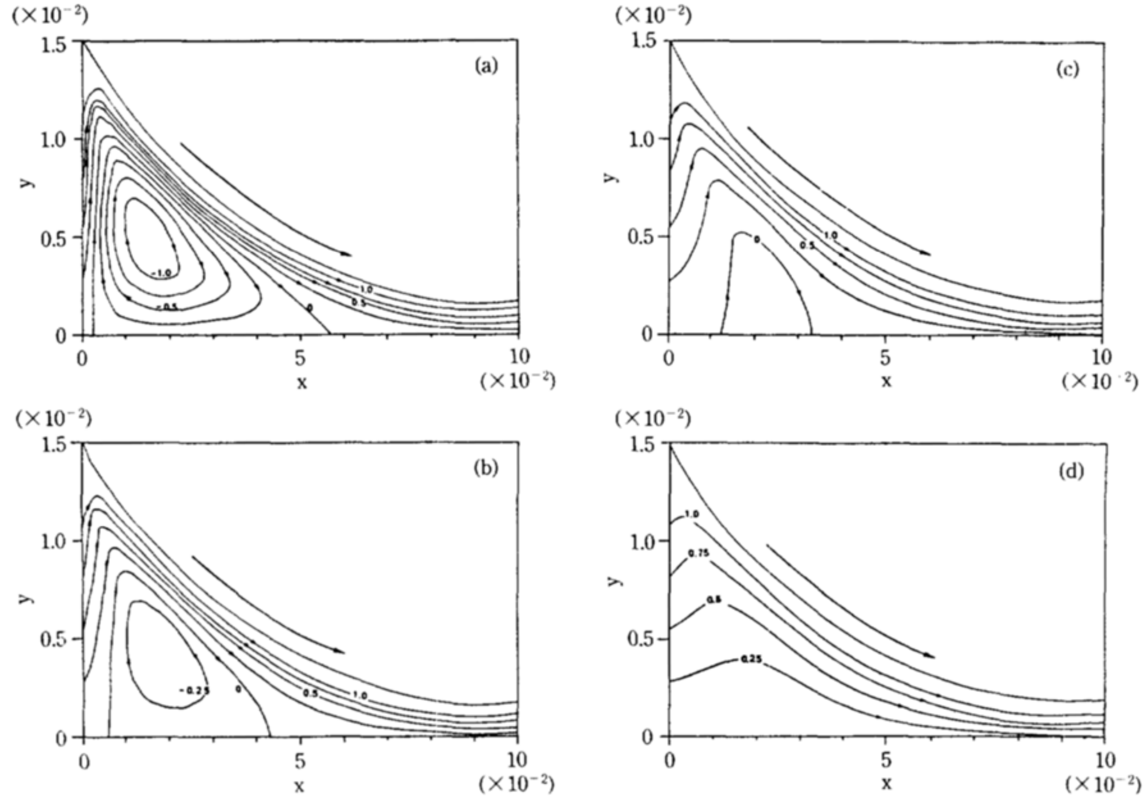

Fig. 4. Predicted streamlines corresponding to Fig. 3.
(a) u_{in}=0.355 m/s, (b) u_{in}=0.555 m/s, (c) u_{in}=0.8 m/s, (d) u_{in}=1.2 m/s.

Fig. 4 shows the contours of streamlines for Fig. 3: on the centre line, two stagnation points may be observed, where u=v=0.

It shows the marked change in the streamline pattern that occurs as the flow rate is increased. The recirculating zone is located immediately downstream of the nozzle and decreases in size as the inlet velocity is increased. Again, the recirculating zone vanishes as the inlet velocity is increased.

The loci of the stagnation points are represented by the dotted lines in Fig. 5. As u_{in} increases, the stagnation points move away from the surface of the roller. It is to be expected that a larger inlet velocity than the rotating roller speed leads to the solidified shell being unbonded at the nip, but too small an inlet flow rate will cause squeezing of solidified metal upstream of the nip.

For stable casting, it is necessary to select operating parameters such that a central recirculating zone will exist. It seems obvious that for proper formation of a central recirculating zone, close control of the casting speed, the inlet flow rate and the roller spacing would be critical.

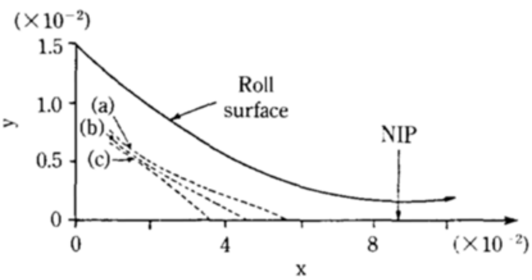

Fig. 5. Predicted stagnation loci corresponding to Fig. 3.
(a) u_{in}=0.355 m/s, (b) u_{in}=0.555 m/s,
(c) u_{in}=0.8 m/s.

In order to obtain a little more insight into the flow in the vicinity of the nip, Fig. 6 shows the evolution of the dimensionless velocity across the gap at the nip position.

In the roller surface regions the metal stream appears to have a jet-like character, implying a high casting speed. The steep velocity gradients are mainly

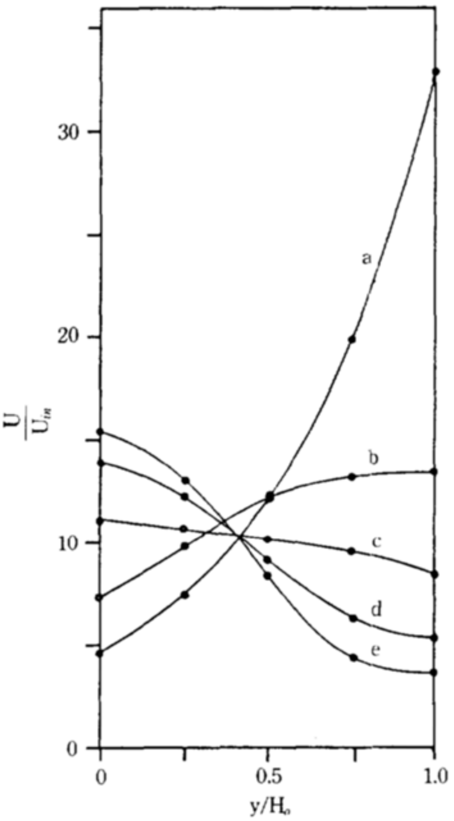

Fig. 6. Calculated velocity profiles at nip for $\Omega=150$ rpm, $W=1.5\times10^{-2}$ m/s and $H_o=1.5\times10^{-3}$ m.
u_{in} =, (a) 0.145, (b) 0.355, (c) 0.555, (d) 0.8, (e) 1.2 m/s.

due to the high roller speed but the role of higher inlet velocities is obvious in flattening out the profiles.

Fig. 7 shows the turbulent kinetic energy distribution within the rotating bank corresponding to various values of the inlet velocity.

It is seen that high levels of turbulence are established in the centre and upper regions in the vicinity of the roll surface of the rotating bank. The turbulent kinetic energy reaches high levels in recirculating regions. On the reverse flow boundary, where the mean velocity is zero, the local turbulence intensity tends to infinity.

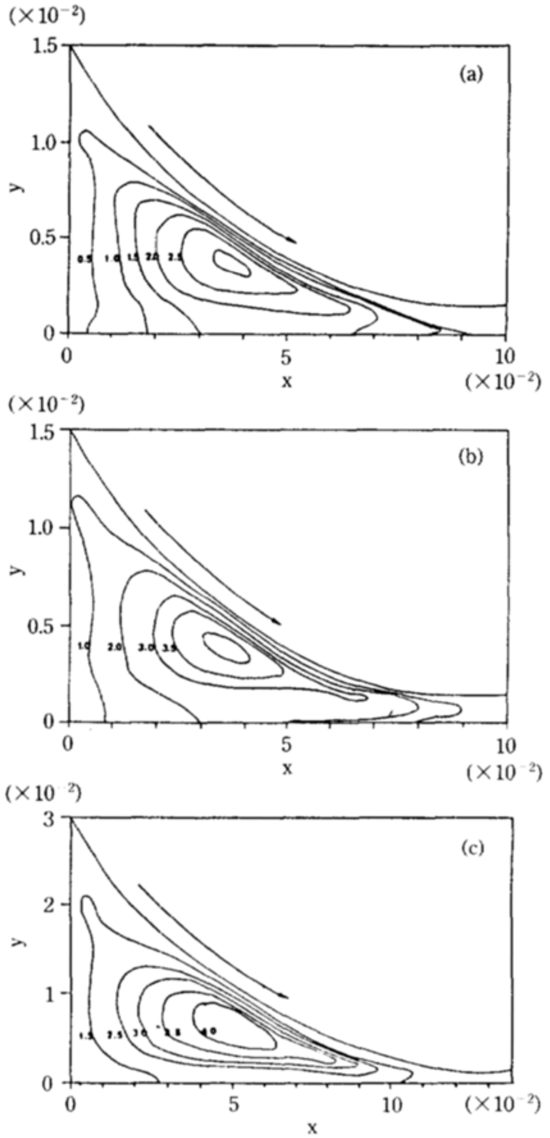

Fig. 7. Predicted turbulent kinetic energy maps corresponding to various operating parameters.
(a) $\Omega=150$ rpm, $W=1.5\times10^{-2}$ m, $H_o=1.5\times10^{-3}$ m and $u_{in}=0.145$ m/s, (b) $\Omega=150$ rpm, $W=1.5\times10^{-2}$ m, $H_o=1.5\times10^{-3}$ m and $u_{in}=0.355$ m/s, (c) $\Omega=150$ rpm, $W=3\times10^{-2}$ m, $H_o=1\times10^{-3}$ m and $u_{in}=0.145$ m/s.

CONCLUSIONS

A mathematical model has been developed to predict the turbulent flow field of a molten metal stream in a twin-roll strip casting process. The computation using the turbulent Navier-Stokes equation and the standard two-equation k-ε turbulence model has been applied, and predicted results are presented, describing the evolution of the turbulence velocity fields and turbulence properties.

(1) The flowfield of the rotating bank between the

twin rollers was successfully simulated by using the turbulence model.

(2) In the turbulent flow field a recirculating zone is located in the vicinity of the middle of the rotating bank of molten metal. The size of the recirculating zone with a fixed geometrical configuration decreases with increasing inlet flow rate.

(3) The predicted turbulent kinetic energy maps for various operating conditions showed the molten metal to be highly turbulent in the vicinity of the roller surface.

(4) Furthermore, extension of this work to a mathematical model including the solidification pattern of the cast strip for the prediction of the end point would make a valuable contribution to more exact computer modelling.

NOMENCLATURE

b : constant (=0.05)
C_1, C_2 : coefficients in k-ε turbulence model
E : friction factor in law of the wall (=9.973)
g : gravitational acceleration [m^3/s]
G_k : generation of turbulent kinetic energy by shear
H : roll spacing coordinate [m]
$\bar{H}$: coordinate of roll spacing ($=H_o/R$)
H_o : half the roll spacing [m]
k : turbulent kinetic energy [m^3/s^2]
P : pressure [$kg/m\ s^2$]
Q : volumetric flow rate [$m^3/m\ s$]
r : coordinate of radius [m]
R : roll radius [m]
R_{ij} : Reynolds stress
u_i, u_j : tensorial notation of turbulent velocity vector [m/s]
u, v : velocities of x and y [m/s]
W : width of nozzle [m]
x : coordinate of axis of casting [m]
$\bar{x}_1$: dimensionless distance ($=x_1/R$)
$\bar{x}_2$: dimensionless distance ($=x_2/R$)
x_i, x_j : tensorial notaion of position vector [m]
y : coordinate of width direction [m]

Greek Letters

Γ : exchange coefficient
ε : dissipation rate of turbulent energy [m^3/s^3]
K : Von Karman's constant (=0.4187)
μ : molecular viscosity [kg/m s]
μ_e : effective viscosity [kg/m s]
μ_t : turbulent viscosity [kg/m s]
ρ : density [kg/m^3]
σ_k : Prandtl/Schmidt number for the turbulent kinetic energy
σ_ε : Prandtl/Schmidt number for the dissipation rate of turbulence
ϕ : instantaneous scalar quantity
Φ : general dependent variable
Ω : rotation speed of roll [rad/min]

REFERENCES

1. Yamauchi, T., Nakanori, T., Hasegawa, M., Yabuki, T. and Ohnishi, N.: *Trans. ISIJ*, **28**, 23 (1988).
2. Dancy, T. E.: *I&SM*, Dec., 25 (1987).
3. Stanek, V. and Szekely, J.: *Metal. Trans.*(B), **14B**, 487 (1983).
4. Miyazawa, K., Choh, T. and Inouye, M.: *J. JIM*, **46**, 1102 (1982).
5. Bessemer, H.: Iron and Steel Institute (London), Autumn Meeting, Oct. 6, 1891, also *J. Metals*, Nov., 1189 (1965).
6. Miyazawa, K. and Szekely, J.: *Metal. Trans.*(A), **12A**, Jun., 1047 (1981).
7. Kraus, H. G.: *Numerical Heat Transfer*, **10**, 63 (1986).
8. Saitoh, T., Hojo, H., Yaguchi, H. and Kang, C. G.: *Metal. Trans.*(B), **20B**, Jun., 381 (1989).
9. Hinze, J. O.: "Turbulence", McGraw-Hill Book, 2 nd ed., New York, 1975.
10. Tennekes, H. and Lumley, J. L.: "A First Course in Turbulence", The MIT Press, Cambridge, MA., 1972.
11. Rodi, W.: "Turbulence Models and Their Applications in Hydraulics-A State of the Art Review", 2nd ed., International Association for Hydraulic Research, Delft, 1984.
12. Launder, B. E. and Spalding, D. B.: *Comp. Meth. Appl. Mech. Engr.*, **3**, 269 (1974).
13. Nallasamy, M.: *Computers and Fluids*, **15**(2), 151 (1987).
14. Anderson, D. A., Tannehill, H. A. and Pletcher, R. H.: "Computational Fluid Mechanics and Heat Transfer", Hemisphere Publishing Co., 1985.
15. Chen, Y. S.: "A Computer Code for Three-Dimensional Incompressible Flows Using Nonorthogonal Body-Fitted Coordinates Systems", NASA CR-178818, Mar., 1986.
16. Patankar, S. V.: "Numerical Heat Transfer and Fluid Flow", McGraw-Hill Book Co., 1980.